

# Dynamic Properties of Microemulsions in the Single-Phase Channels

Lukas Wolf,<sup>\*,†</sup> Heinz Hoffmann,<sup>†</sup> Walter Richter,<sup>‡</sup> Takashi Teshigawara,<sup>§</sup> and Tohru Okamoto<sup>§</sup>

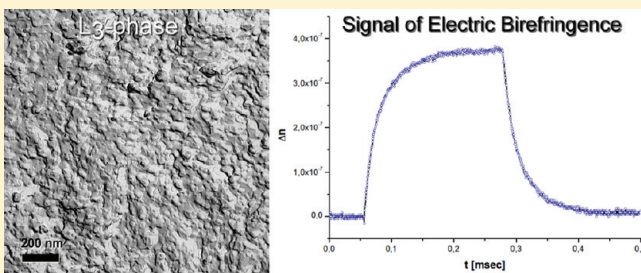
<sup>†</sup>University of Bayreuth, BZKG and BayColl, Gottlieb-Keim-Str. 60, 95448 Bayreuth, Germany

<sup>‡</sup>Friedrich-Schiller-University, Centre for Electron Microscopy, Ziegelmühlenweg 1, 07743 Jena, Germany

<sup>§</sup>Shiseido Research Center, 2-2-1 Hayabuchi, Tsuzuki-ku, Yokohama, Japan 224-8558

 Supporting Information

**ABSTRACT:** We have studied the dynamic and rheological properties in the single-phase channels of a microemulsion system with a mixed anionic/nonionic surfactant system and decane from the aqueous to the oil phase. One isotropic channel, called the “upper” channel, begins at the L<sub>3</sub> phase (sponge-like phase) of the binary surfactant mixture on the water side and passes with a shallow minimum for the surfactant composition to the oil side. The other “lower” single-phase channel begins at the micellar L<sub>1</sub> phase and ends in the middle of the phase diagram. Both isotropic channels are separated by a huge anisotropic single phase L<sub>α</sub> channel that reaches from the water side to 90% of oil in the solvent mixture. The structural relaxation time of the viscous fluids could be measured with electric birefringence (EB) measurements, where a signal is caused by the deformation of the internal nanostructure of the fluids by an electric field. For the L<sub>3</sub> phase, the EB signal can be fitted with a single time constant. With increasing oil in the upper channel, the main structural relaxation time passes over a maximum and correlates with the viscosity. Obviously, this time constant controls the viscosity of the fluid ( $\eta^0 = G' \cdot \tau$ ). It is remarkable that the longest structural relaxation time increases three decades, and the viscosity increases two decades when 10% of oil is solubilized into the L<sub>3</sub> phase. Conductivity data imply that the fluid in the upper channel has a bicontinuous structure from the L<sub>3</sub> phase to the microemulsion with only 10% oil. In this oil range, the conductivity decreases three decades, and the electric birefringence signals are complicated because of a superposition of up to three processes. For higher oil ratios, the structure obviously changes to a HIPE (high internal phase emulsion) structure with water droplets in the oil matrix.



## INTRODUCTION

Microemulsions are thermodynamically stable phases from oil, water, and surfactants.<sup>1</sup> The phases contain well-defined structures, such as oil droplets in a continuous water phase, water droplets in a continuous oil phase, and bicontinuous structures. The detailed structures depend on the composition of the system in the ternary phase diagram. Usually, the structures change with a change in the composition of the samples. For many years, microemulsions with ionic surfactants were in the focus of interest.<sup>2</sup> More recently, microemulsions with nonionic surfactants have become the center of interest.<sup>3</sup> As a consequence, we now have a good understanding of microemulsions. It is known, for example, how the phases can be optimized for as little surfactant as possible and how the surfactant can be optimized for a given oil. Of fundamental importance for the understanding of the systems is the value of the interfacial tension of a micellar solution against an oil phase.<sup>4</sup> For a high solubilization of an oil in a micellar solution, the interfacial tension has to be minimized.<sup>5</sup> One of the most fascinating features of nonionic microemulsions is isotropic single-phase channels that pass from the aqueous micellar phase continuously to the oil phase for constant surfactant concentration.<sup>6</sup> Because of SANS and SAXS, we have a good understanding of the structures in these channels. Many

systems have been investigated that have two channels from the water to the oil side, one at lower temperature and one at a higher temperature, and a single channel in the middle of the phase diagram that is connected with the two channels at both sides.<sup>7</sup> Today, there is a good theoretical understanding of the structures in the isotropic channels and about the thermodynamics of microemulsions with nonionic surfactant. However, very few investigations have been carried out on the dynamic behavior of the microemulsions, and no systematic investigation has so far been made in a channel from the water side to the oil side.

In this investigation, we therefore will study the dynamic properties of microemulsions in the single-phase channels by rheology and the electric birefringence method. The measurements were carried out on a system with an anionic/nonionic surfactant mixture that was similar to one that was previously studied and from which we knew the position of the single phase channels.<sup>8</sup>

**Received:** April 20, 2011

**Revised:** August 15, 2011

**Published:** August 15, 2011

## ■ EXPERIMENTAL SECTION

**Materials.** The nonionic surfactant iso-tridecyl-triethylenglycolether, abbreviated as IT 3, was obtained from the Sasol Company (Hamburg, Germany) (“Marlipal O13/30”). This compound has a polydisperse distribution of EO groups with an average of three EO units. Sodium dodecyl sulfate (SDS, cryst. research grade) was purchased from the Serva Company (Heidelberg, Germany).  $MgCl_2 \cdot 6 H_2O$  was purchased from the Grüssing Company (Filsum, Germany). N-Decane (analytical grade) was obtained from the Merck Company (Darmstadt, Germany).

**Preparation of  $Mg(DS)_2$ .** For the preparation of  $Mg(DS)_2$ , 400 mM SDS solution was mixed with 200 mM  $MgCl_2$  solution under stirring. The bivalent counterion  $Mg^{2+}$  binds stronger to the dodecyl sulfate than the sodium ion, leading to a precipitation of  $Mg(DS)_2$  in solution below its Krafft temperature around 25 °C. The solution was heated above 25 °C to obtain a clear solution and then cooled to 20 °C. After precipitation overnight,  $Mg(DS)_2$  was filtered and washed several times with deionized water to remove excess salt. The purity of the surfactant thus could be checked by measuring the conductivity of the flow through of the filtered  $Mg(DS)_2$ . The washed  $Mg(DS)_2$  was freeze-dried with the freeze-drying device Alpha 1-4, Christ Company (Osterode, Germany), and used without further purification.

**Preparation of Samples.** All samples were prepared by weighing the components directly in test tubes on an analytical balance. The test tubes were sealed with Teflon tape, tempered at 25 °C in a water bath, and vortexed several times thoroughly. All samples were incubated at least 3 days at 25 °C before being investigated for their phase behavior. In general, a phase diagram was scanned with a resolution of 5% in the composition of the mass fraction of IT 3 and decane. Finer steps were investigated in the beginning of the narrow upper single-phase channel. The multiphase samples were viewed and imaged without and in between crossed polarizers to visualize the birefringence of lamellar regions.

**Freeze-Fracture Transmission Electron Microscopy (FF-TEM).** The microemulsions, prepared in presence of 20% (w/w) glycerin in the aqueous phase were stored at room temperature (25 °C) and quick-frozen from RT using the sandwich technique. A small amount of the samples was sandwiched between two copper profiles (BAL-TEC/Balzers, Liechtenstein) as used for the double-replica technique and frozen by plunging these sandwiches immediately into a liquefied ethane–propane mixture (v/v 1/1) cooled in liquid nitrogen. Fracturing and replication were performed at –150 °C in a BAF 400T freeze-fracture device (BAL-TEC/Balzers, Liechtenstein) equipped with electron guns and a film sheet thickness monitor. For replication, at first, Pt(C) was evaporated under an angle of 35° (thickness: 2 nm), followed by C under 90° angle (thickness 20 nm). The replicas were placed on electron microscopic copper grids (Mesh 400), cleaned by chloroform–methanol mixture (v/v 2/1), and examined in an EM 900 electron microscope (Zeiss, Oberkochen, Germany).

**Conductivity and Rheology Measurements.** For conductivity measurements, we used the microprocessor conductivity meter LF3000 from the WTW Company (Weilheim, Germany). The rheology was measured with the cone–plate rheometer RheoStress 600 from the Haake Thermo Scientific Company (Karlsruhe, Germany). All samples were investigated at 25 °C.

**Electric Birefringence Measurements.** The electric birefringence device is a self-made device with a 632.8 nm He–Ne laser, crossed polarizers, aperture plates, a Kerr cell with temperature control, and a photomultiplier. For the generation of an electric pulse, there was used the Cober “high power pulse generator” model 606. The signal of the photomultiplier was recorded with the Voltcraft DSO-2090 USB-oscilloscope. Data were processed and evaluated with the computer software “Origin”.

**SANS Measurements.** For SANS measurements, samples were prepared with  $D_2O$  instead of  $H_2O$ . By replacing  $H_2O$  by  $D_2O$ , the phases in the single-phase channels are slightly shifted. To obtain transparent isotropic phases, we had to adjust the surfactant composition by increasing the mass fraction of IT 3 by ~2%. SANS data were obtained with the SANS device D11 at the Institut Laue-Langevin in Grenoble, France. Samples were filled in 1 mm quartz cuvette (Helma), and temperature was set to 25 °C.

Evaluation of data (background detection, subtraction of signal intensity, scaling of data) was performed with standard computer software.

## ■ RESULTS AND DISCUSSION

**Phase Diagram  $Mg(DS)_2/IT\ 3-H_2O/n$ -Decane.** On microemulsion systems with a single nonionic surfactant, it is not possible to pass from a single aqueous phase to a single oil phase at constant temperature. The interfacial tension of nonionic surfactants changes with temperature, and thus the single-phase regions of microemulsions are temperature-dependent. The amphiphilic properties of surfactants can also be changed by adding a cosurfactant to the surfactant solution. In the present investigation, we therefore chose a binary mixture of a hydrophilic surfactant with a lipophilic surfactant. For the ionic surfactant, we chose the  $Mg^2$  salt of SDS.  $Mg(DS)_2$  is more lipophilic than SDS, reduces the surface tension more effectively, and is known to form liquid crystalline  $L_\alpha$  phases when mixed with suited cosurfactants.<sup>8</sup> As lipophilic cosurfactant, we used iso-tridecyl-triethylenglycolether (abbreviation IT 3, =  $C_{13}E_3$ ). By changing the mass fraction of the two molecules in the surfactant solution, it turned out to be possible to pass from a micellar  $L_1$  phase with only  $Mg(DS)_2$  over lamellar  $L_\alpha$  and an  $L_3$  phases (sponge-like phase) with the surfactant mixtures to an  $L_1/L_2$  ( $L_2$  = inverse micellar phase) two phase situation for the solution with pure IT 3. The phase sequence of the binary surfactant mixture is shown in Figure SI1 of the Supporting Information, and detailed rheological investigations can be found in Figure SI2 of the Supporting Information. Some nonionic surfactants show the same sequence of phases with increasing temperature.

The plot of the surfactant mixture against the mass fraction  $x$  of the oil decane in the solvent mixture between 0 and 1 is shown in Figure 1. The total surfactant concentration was kept constant at 15% (w/w), the temperature was kept at 25 °C, and samples were prepared with 20% glycerine in  $H_2O$  for possible FF-TEM investigations to prevent freezing artifacts.

The phase diagram contains two isotropic channels, a lower one and an upper one. The upper one begins on the surfactant axis at the region of the  $L_3$  phase. With increasing oil, the channel first shifts to a lower IT 3 ratio and then again to a higher IT 3/ $Mg(DS)_2$  ratio for higher oil ratios. It ends on the oil side at 80% decane and pure IT 3 as surfactant. The lower channel begins at

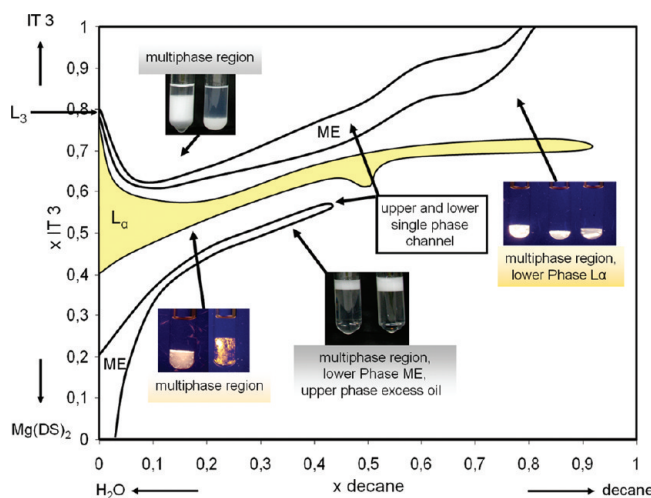


**Figure 1.** Phase diagram of system  $\text{Mg}(\text{DS})_2/\text{IT } 3-\text{H}_2\text{O}/\text{decane}$  at 15% (w/w) surfactant and 25 °C, 20% glycerin in  $\text{H}_2\text{O}$   $\times \text{IT } 3$  = mass fraction of IT 3 in the surfactant mixture,  $x$  decane = mass fraction of decane in the solvent mixture. “ME” indicates isotropic microemulsion area, and  $L_a$  indicates area of anisotropic lamellar channel.

the  $L_1$  region and ends in the middle of the phase diagram at an IT 3 ratio of 0.57.

Both channels are separated by a huge single-phase birefringent  $L_a$  region that extends from 0 to 90% decane with slightly increasing mass fraction of IT 3. All samples in the  $L_a$  channel behave like gels. However, the storage modulus  $G'$  is decreasing constantly with increasing oil content, indicating that the gels become softer. Pictures of the  $L_a$  phases between crossed polarizers at different temperatures and detailed rheology data can be found online in Figure SI3 of the Supporting Information.

A significant feature of the  $L_a$  channel is its high-temperature stability. Samples between  $x$  decane = 0 to 0.9 are stable at least between 10 and 40 °C, and samples with  $x$  decane 0 to 0.4 are even stable at least up to 60 °C. Although the  $L_a$  channel is quite narrow, its high-temperature stability is amazing. This feature is obvious due to the surfactant mixture, where the hydrophilic–lipophilic balance is determined more by the mass fraction of the cosurfactant than by the temperature.  $L_a$  phases with oil and a single nonionic surfactant of the type  $C_i\text{E}_j$  are not so stable.<sup>32</sup>

The microemulsions in the lower single phase channel are transparent phases that show no flow birefringence under shear. The samples in the upper phase channel have somewhat different properties. Whereas the  $L_3$  phase without decane is completely transparent, the samples with decane look somewhat bluish and their scattering intensity is most intensive around  $x$  decane 0.03 and 0.1. For higher oil content, the scattering intensity is decreasing again. Pictures of samples from the lower and upper single phase channel are shown in Figure SI4 of the Supporting Information. The different macroscopic properties in the upper and lower phase channels for the same amount of oil are already an indication that the structures in the two single-phase channels are different. In many previous publications of microemulsions, it was shown that the micellar structures in a single-phase channel varied from o/w droplets to bicontinuous structures to w/o structures.<sup>9</sup>

The following chapters will show, that the situation in the present system must be different and more complicated. It

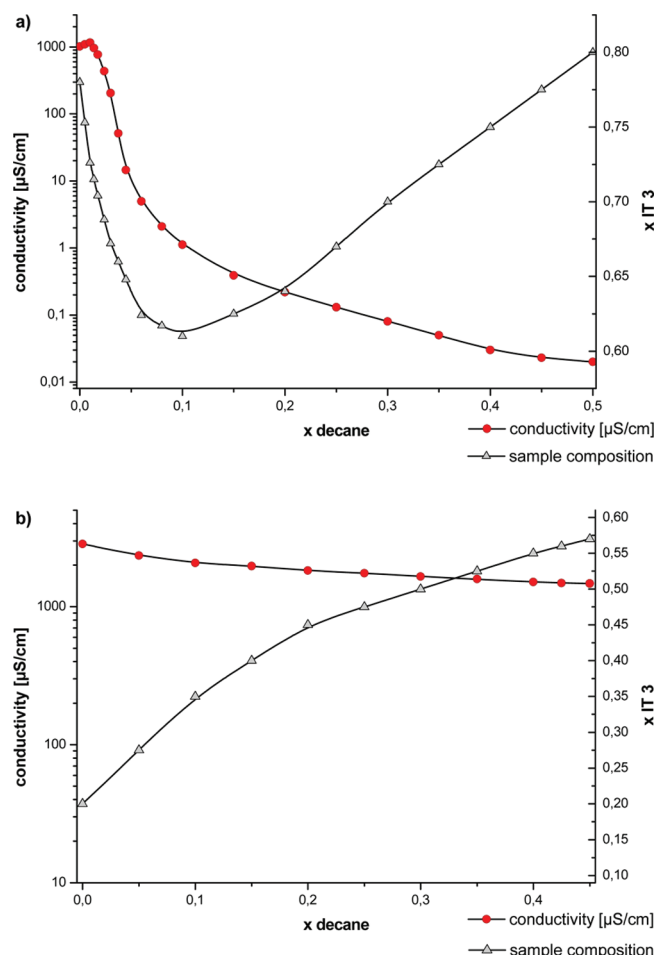


**Figure 2.** Plot of conductivity (red dots) and IT 3 content (gray triangles) against mass fraction of decane in solvent mixture. (a) Conductivity data for the upper single phase channel. (b) Conductivity data for the lower single phase channel.

should, however, be clear that the situation in nonionic and in somewhat ionically charged systems may be somewhat different. Our investigated system is the first system with an ionic surfactant for which the ionic charge was not shielded by excess salt that forms an isotropic channel from the water side to the oil side.

**Conductivity in the Single-Phase Channels.** The plot of the conductivity in the upper and lower single-phase channels against the mass fraction of decane in the solvent mixture is shown in Figure 2.

In the upper channel, the conductivity first increases slightly from  $\sim 1000 \mu\text{S}/\text{cm}$  of the sample without decane to  $1160 \mu\text{S}/\text{cm}$  to the sample with 1% decane. The reason for this lies in the change of the composition of the surfactant mixture. In the range from 1 to 10% decane, the conductivity decreases abruptly three orders of magnitude to  $1 \mu\text{S}/\text{cm}$  even though the fraction of the anionic  $\text{Mg}(\text{DS})_2$  is increasing. For higher mass fractions of decane, the conductivity values decrease continuously to low values as, for example,  $0.03 \mu\text{S}/\text{cm}$  for the sample with a water/oil ratio of 1/1 (w/w). The conductivities thus indicate a dramatic change in the nanostructure of the upper channel with solubilization of small amounts of oil into the  $L_3$  phase. The abrupt collapse of the conductivity indicates that the system

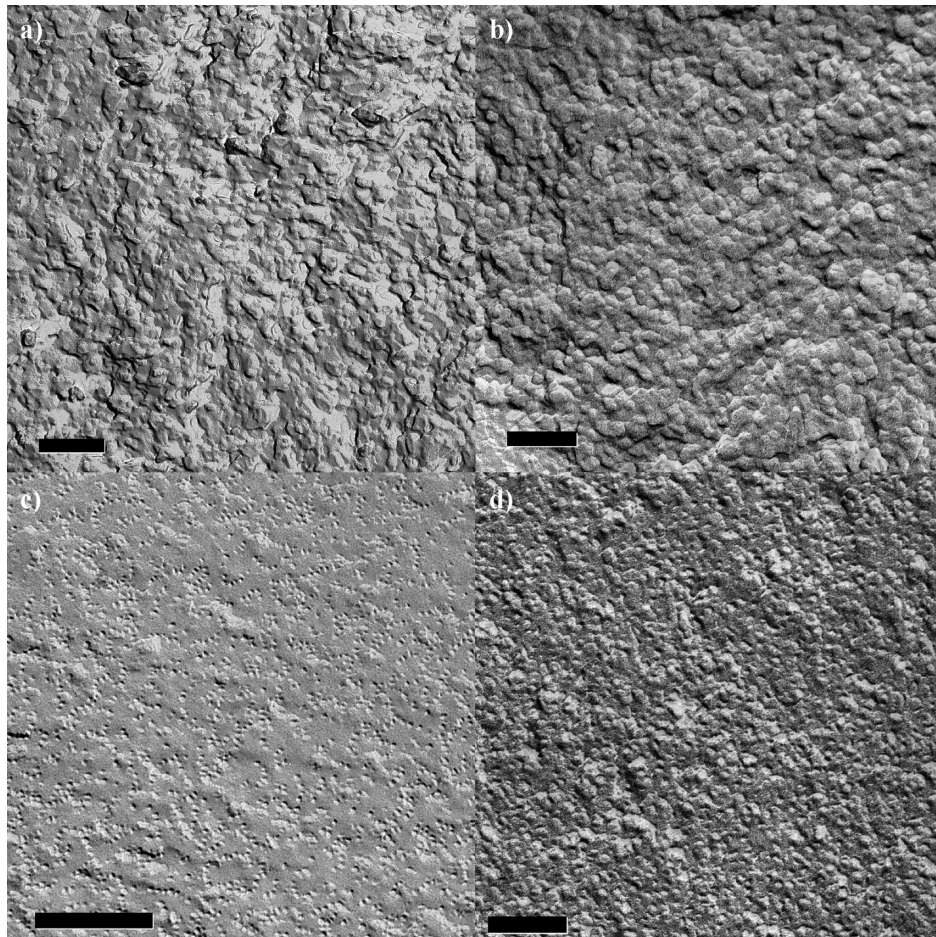


**Figure 3.** FF-TEM micrographs with 15% (w/w) surfactant  $\text{Mg}(\text{DS})_2/\text{IT } 3$ , 20% glycerine in  $\text{H}_2\text{O}$ , prepared at 25 °C; scale bar = 200 nm. (a)  $\text{L}_3$  phase without oil at  $x \text{ IT } 3 = 0.79$ , (b) microemulsion of upper channel with  $x \text{ IT } 3 = 0.67$ ,  $x$  decane = 0.2, (c) microemulsion of lower channel with  $x \text{ IT } 3 = 0.35$ ,  $x$  decane = 0.1, o/w-structure, droplet size ~7 nm, and (d) microemulsion of lower channel with  $x \text{ IT } 3 = 0.45$ ,  $x$  decane = 0.2, droplet size ~14 nm.

changes from a bicontinuous structure to a w/o structure (water-in-oil). Conductivities in the isotropic channels of microemulsions from nonionic surfactants have been reported in the literature.<sup>10</sup> In such systems, the conductivity in the upper channel decreases continuously with increasing oil content. These measurements have helped to establish the view that we have today from the structures in the upper channel. With increasing oil content, the bicontinuous  $\text{L}_3$  phase swells with the solubilized oil between the bilayers and is finally transformed at high oil content to a w/o system. With equal amount of oil and water, SAXS data and conductivities show that this phase is still a bicontinuous phase.<sup>11</sup> Our conductivity data unambiguously show that the structures in the upper channel of the investigated system are different from the structures of known systems with nonionic surfactants. We find a rather abrupt transition from the bicontinuous  $\text{L}_3$  structure to a w/o structure with only 10% of oil in the solvent mixture.

The conductivity data of the lower channel indicate that the nanostructure in the lower channel does not change much with increasing oil in contrast with the nanostructure in the upper channel. At the water corner, the conductivity in the lower channel with 2900  $\mu\text{S}/\text{cm}$  is much higher than the conductivity of the  $\text{L}_3$  phase of the upper channel with 1000  $\mu\text{S}/\text{cm}$ . The reason for this is that the  $\text{Mg}(\text{DS})_2$  concentration is much higher in the lower channel. With increasing oil content, the

conductivities decrease slightly to 1500  $\mu\text{S}/\text{cm}$  at the middle of the phase diagram, which is where the channel ends. The reason for the decrease is mainly the decreasing mass fraction of  $\text{Mg}(\text{DS})_2$ . Obviously, the lower channel consists of a continuous water phase in which oil droplets are dispersed (o/w structure).

As already mentioned, the lower and upper single-phase channels are not connected to each other in contrast with the classical microemulsion systems with single nonionic surfactant and hydrocarbons. In the present system, both channels are separated by a large single anisotropic  $\text{L}_\alpha$  channel.

A plot of the conductivity in the  $\text{L}_\alpha$  channel can be found in Figure SI4 of the Supporting Information. The conductivity on the water-side is ~400  $\mu\text{S}/\text{cm}$  and decreases with increasing oil content and increasing  $x \text{ IT } 3$  constantly to a value of 40  $\mu\text{S}/\text{cm}$  at the  $\text{L}_\alpha$  phase with 90% decane. It is noteworthy that the sample without decane at the water side has a lower conductivity than the  $\text{L}_3$  phase despite the fact that it contains ~60% more anionic  $\text{Mg}(\text{DS})_2$  and also a much lower conductivity than the microemulsion from the lower single-phase channel with the same  $x \text{ IT } 3$  value of 0.5. This already indicates that the structure consists of densely packed multilamellar vesicles, where the conductivity is low due to the limited movement of the ions.<sup>12</sup>

**FF-TEM Micrographs in the Upper Channel.** An FF-TEM micrograph of the  $\text{L}_3$  phase without oil is shown in Figure 3a. In this technique, the replica of a fractured plane across the sample is

reproduced. From previous investigations with this technique, it is known that the fracture follows the midplane of the bilayers.<sup>13</sup> One can see a highly structured surface in which the smallest objects that can be identified have dimensions between 10 and 20 nm. In many parts of the micrographs, it is possible to identify globular white domains that are surrounded by a gray ring. These are typical features of the L<sub>3</sub> phase where the fracture plane has cut through a tubular bilayer. The dimensions of these globular spots correspond to the size that is detected from the correlation peak in scattering measurements and which is close to the interlamellar distance in the neighboring L<sub>a</sub> phase.<sup>14</sup> The typical dimensions that are observed from the Cryo-TEM and the FF-TEM micrographs are the same and give a consistent picture. In Figure 3b, an FF-TEM micrograph from a sample is shown that contains 20% oil in the solvent mixture. The micrograph of the microemulsion with 20% decane looks different than the micrograph of the L<sub>3</sub> phase without oil. Now densely packed globular particles can be seen with an average diameter of 40–50 nm. The FF-TEM micrographs support the assumption of the conductivity measurements that the bicontinuous structure of the L<sub>3</sub> phase is transformed to a w/o droplet structure with little oil.

Such w/o structures of a similar system were already successfully imaged with help of the Cryo-TEM method.<sup>15</sup> The droplet size is also consistent with the calculated size of 46 nm that can be obtained by the simple core–shell model.

Micrographs of samples from the lower single-phase channel with 10 and 20% decane in the solvent mixture are shown in Figure 3c,d. The micrographs show tiny droplets with a diameter of ~7 nm for the sample with 10% decane and ~14 nm for 20% decane that are randomly distributed in the surrounding matrix that is water. The droplet size for both samples also fit perfectly with the core–shell model.

**Electric Birefringence Measurements in the Upper Single-Phase Channel.** Electric birefringence measurements are usually carried out on colloidal systems to determine the dimension of particles and aggregates and to determine the optical anisotropy of these structures.<sup>16</sup> The method has been used to determine the persistence length of polyelectrolytes and polymers,<sup>17</sup> of worm-like micelles,<sup>18</sup> of pieces of DNA,<sup>19</sup> and so on. Good signals were also obtained on L<sub>3</sub> phases.<sup>20</sup> At the time of the measurement, it had not been unambiguously clear whether L<sub>3</sub> phases had a bicontinuous structure or were a solution of discrete disk-like micelles.<sup>21</sup> It was assumed that the signals were due to the orientation of the disk-like particles in the electric field. The orientation time was therefore used to calculate the diameter of the disk-like aggregates. The results gave diameters that corresponded to the interlamellar distance of the L<sub>a</sub> phase that is next to the L<sub>3</sub> phase. These results could also explain the low viscosity of the L<sub>3</sub> phases. Later measurements on L<sub>3</sub> phases, in particular, FF-TEM measurements, showed that L<sub>3</sub> phases have a bicontinuous structure.<sup>22</sup> The electric birefringence signals have then to be explained by the deformation of these structures in electric fields. In both interpretations, the alignment of disk-like particles or the deformation of the L<sub>3</sub> structure solvent molecules has to diffuse over the length of the dimension of the structure, and it is not possible from the signal what the origin of the signal is.<sup>23</sup> The results lead, however, to a structural relaxation time that controls the macroscopic dynamic properties of these phases. The electric birefringence method was therefore used to determine the structural relaxation times in microemulsions and, in particular, in the single-phase channel of this system for which we had determined first the phase diagram. According to our knowledge,

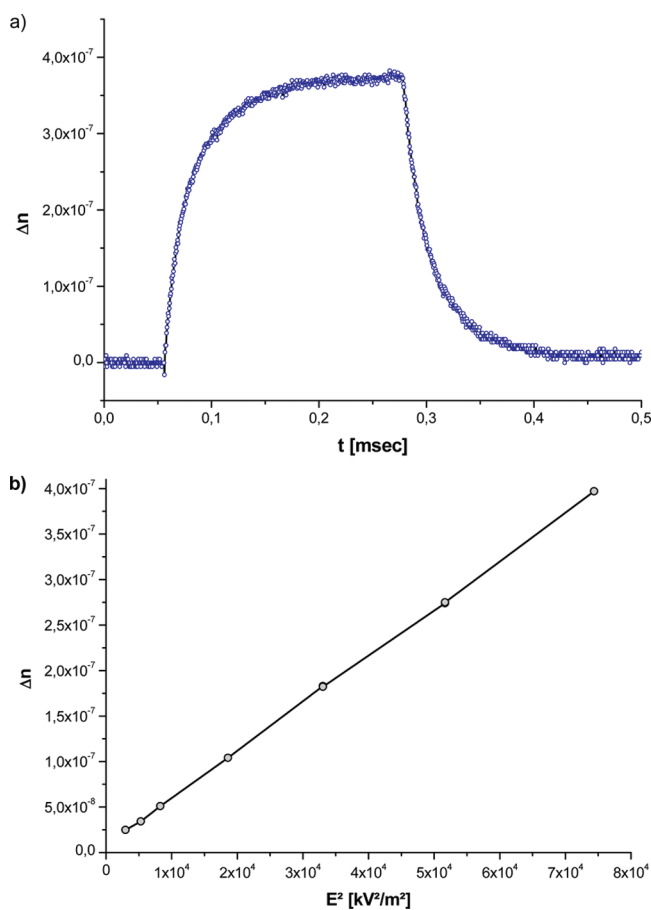


**Figure 4.** (a) EB signal of the L<sub>3</sub> phase. Sample composition: 15% (w/w) surfactant,  $\alpha$  IT 3 0.79, 20% glycerine in H<sub>2</sub>O. Signal recorded at an field strength  $E$  of 273 kV/m. (b) Plot of  $\Delta n$  against  $E^2$ .  $\Delta n$  increases linearly with  $E^2$  and therefore follows Kerr's law.

these are the first measurements of the dynamic behavior of microemulsions in the single-phase channel.

We would like to note that electric birefringence measurements have been carried out on microemulsions of the system C<sub>12</sub>E<sub>5</sub>/H<sub>2</sub>O/n-octane.<sup>24</sup> The measurements were done in the lower isotropic channel from the water side to the upper channel on the oil side. Signals with a single relaxation time were observed. The time constants showed two maxima with the oil constant at 30 and 70% of n-octane and a minimum in between the maxima at 50% of oil. The Kerr constant showed a broad maximum at ~50% of oil. Whereas it was not tried to interpret the results with a model in a quantitative way, the results were consistent with the generally accepted model according to which the structures along the channel developed from o/w droplets over a bicontinuous structure to w/o droplets. The results for the presently investigated system are very different, as will be shown.

In Figure 4a an electric birefringence signal of the L<sub>3</sub> phase is shown. The signal is a simple signal; that is, both the buildup and the decay of the birefringence can be fitted with a single relaxation time that is the same for the buildup and the decay. The birefringence amplitude follows Kerr's law, as is shown in Figure 4b.

This result is most remarkable because it could have been imagined that the amplitude saturates with increasing filed strength or that the bilayers break at high fields. The structural

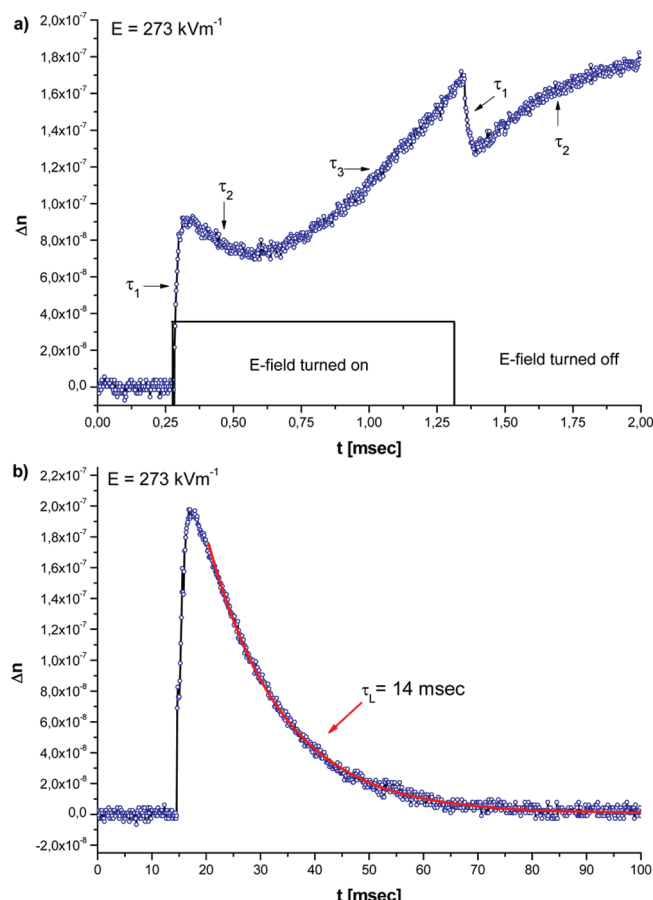


**Figure 5.** EB signal for a microemulsion of the upper single phase channel with 6% decane in the solvent mixture. (a) Signal shown with time sweep of 2 ms and (b) signal with time sweep of 100 ms, longest relaxation  $\tau_L = 14 \text{ msec}$ . The signal identifies three different relaxation processes. Duration of electric pulse = 1 ms.

relaxation time depends on the concentration of the surfactant. It scales with a power exponent of the concentration of  $-3$  ( $\tau \approx (c/c^*)^{-3}$ ).<sup>25</sup> The result is due to the fact that the typical dimension of the  $L_3$  phase scales as for a  $L_\alpha$  phase with the volume fraction with the exponent  $-1$ .

In a general sense, it is very unusual and remarkable that a structural relaxation time for a surfactant phase or for a polymer solution becomes shorter with increasing concentration as for the  $L_3$  phase.

In most situations, the structural relaxation time becomes longer either because of the increasing interaction between the aggregates or because the aggregates become larger as for wormlike micelles in  $L_1$  phases.<sup>26</sup>

Electric birefringence signals were recorded in the same way as for the  $L_3$  phase for the microemulsions with increasing oil content. It was assumed that the shape of the signals would not remain the same as that for the  $L_3$  phase and the time constant and the amplitude would change because the conductivity measurement and FF-TEM images had shown that the bicontinuous structure of the  $L_3$  phase drastically changes when only a little amount of oil is solubilized. The results revealed that this is indeed the case. The signals became very complicated with increasing solubilization of oil, as is shown in Figure 5 for a sample with 6% oil.

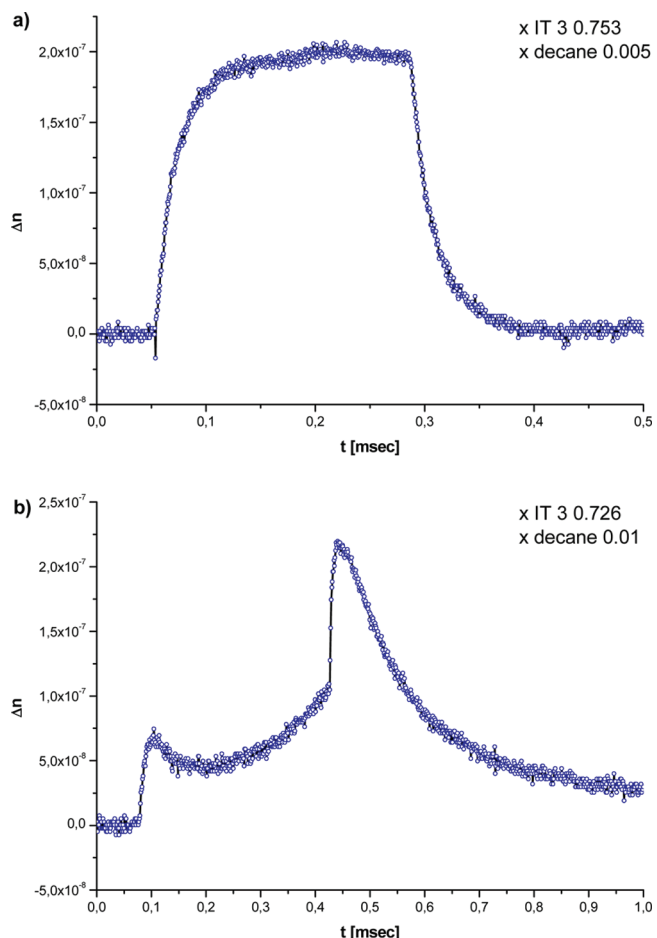


**Figure 6.** EB signals of microemulsion from upper single phase channel. (a) Simple signal with  $x$  decane 0.05. (b) Complicated signal with  $x$  decane 0.01.

Signals that were recorded for different field strength are shown in Figure SI6 of the Supporting Information. As is evident from the individual signals, the signals do not depend on the field strengths.

As is obvious from Figure 5a, the signal seems to indicate a superposition of three separate processes for a pulse of 1 msec duration. The first process, which is indicated as  $\tau_1$  in the Figure, has a relaxation time of  $\sim 15 \mu\text{s}$ . The second one, which opposes the first one, has a relaxation time around  $150 \mu\text{s}$  ( $\tau_2$ ), and the next one ( $\tau_3$ ) has a relaxation time of  $\sim 600 \mu\text{s}$ . When the field is turned off, all three processes are visible again. The last and longest process, indicated as  $\tau_L$  in Figure 5b, has the largest relaxation time of  $\sim 14 \text{ ms}$ . It is remarkable and strange that the signal increases again during the second process to an even higher birefringence level as with the field left on. Similar complicated signals have been observed for electric birefringence measurements on dispersion of clay particles.<sup>27</sup> The complicated signals in these systems are due to the fact that a fraction of the particles align parallel to the electric fields, whereas another fraction aligns perpendicular to the field. The complicated signals will be discussed in a later section. We would like to emphasize here that the main signal that is also the longest process relaxes with a relaxation time that is  $\sim 14 \text{ ms}$  that is much longer than the electric pulse, which is applied only for 1 ms.

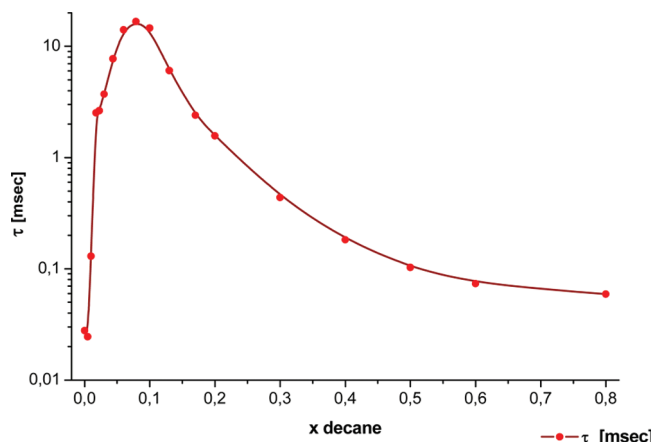


**Figure 7.** Plot of the longest relaxation time  $\tau$  of microemulsions in the upper single-phase channel against the mass fraction of decane in the solvent mixture.

In Figure 6, EB signals of microemulsions from the upper single-phase channel with 0.5% decane and 1% decane in the solvent mixture are shown.

While the signal of the microemulsion with 0.5% decane in the solvent mixture is the same as the signal of the  $L_3$  phase, one can see clearly that the signal with 1% decane becomes already very complicated. EB signals of microemulsions of the upper channel between 0.5 and 10% decane are shown in Figure SI7 of the Supporting Information, and signals for microemulsions from 17 to 80% decane are shown in Figure SI8 of the Supporting Information. Whereas the EB signals of microemulsions with up to 10% decane are very complicated and show a superposition of several processes, the signal becomes simpler again with further increasing oil concentration.

The longest relaxation time can easily be evaluated from all signals because the shorter relaxation processes have already relaxed to zero and need not to be considered during the evaluation of the longest process. A plot of the longest relaxation time against the oil content of the microemulsion is shown in Figure 7. Because of the larger changes of the time constant, a log scale has been used for the time constants. The plot shows a steep maximum for microemulsions around 10% of oil. The relaxation time increases four orders of magnitude.

From a general point of view on solubilization of oil in micellar phases, it is remarkable that the structural relaxation time is increasing with the oil content. For  $L_\alpha$  phase and for entangled wormlike micelles, the structures usually become more flexible with solubilization and the time constants decrease.

As conductivity data already implied, there must be a complex transition mechanism from the bicontinuous  $L_3$  phase to a w/o-HIPE structure with only  $\sim 10\%$  oil. The complicated signals for microemulsions with low oil content are obviously related to this transition mechanism. For higher oil content above 10% oil, EB signals become less complicated. This indicates that the structural transition is complete. The structural relaxation time then is decreasing again because of the decreasing droplet size of the w/o droplets with increasing oil content.

**Rheology in the Upper Single Phase Channel.** It is generally assumed that microemulsions are low viscosity Newtonian fluids. Systematic investigations of the rheological behavior of microemulsions do not seem to have been carried out in the past.

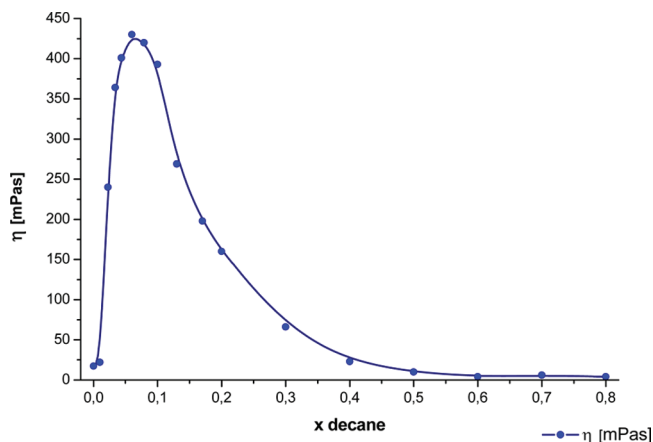


**Figure 8.** Zero shear viscosity  $\eta$  of samples of the upper single-phase channel against the mass fraction of decane.

The kinematic viscosity  $\nu$  of the well-studied system  $H_2O/n$ -octane/ $C_{12}E_5$  has already been investigated along the isotropic channel.<sup>28</sup> The viscosity showed a relatively complicated behavior with two maxima and a minimum at an oil/water ratio near one. The first maximum was  $\sim 20\%$  of oil. The total reported change of  $\nu$  between 10 and 90% of oil was only a factor 10. There was no effort made to explain the two maxima as a function of the oil concentration. The measurements were carried out with an Ubbelohde viscometer, assuming that the fluids were Newtonian fluids. Microemulsions are structured fluids, and they should therefore show a shear thinning behavior. We therefore made rheological measurements of the microemulsions along the isotropic channel from the  $L_3$  phase to the oil phase. The viscosities were measured with a cone/plate viscometer, and it was hoped that the structural relaxation times also could be determined.

The zero-shear viscosity  $\eta^0$ , plotted against the oil content, is shown in Figure 8. The results show a strong maximum of the viscosity around 6–10% of oil. The viscosity at the maximum is almost three orders of magnitude higher than the viscosity of water or of the used oil and about two orders of magnitude higher than the viscosity of the  $L_3$  phase. In comparison with solubilization results of oil into other micellar phases, it is surprising that small amounts of oil into the  $L_3$  phase increase the viscosity so much. Solubilization of oil into an  $L_1$  phase from wormlike micelles and solubilization of oil into the bilayers of a  $L_\alpha$  phase usually leads to the decrease in the viscosity.

Whereas the rise of the viscosity could be rationalized with the increasing correlation length between the  $L_3$  phase and the microemulsions with 10% of oil, the decrease in the viscosity with further increasing oil concentration is unclear. As seen from conductivity results, the microemulsion with 50% of oil consists of water droplets in an oil matrix. Such a phase should have a low viscosity that should be given by the Stokes–Einstein equation

$$\eta = \eta_s(1 + 2.5\phi)$$

where  $\eta_s$  is the viscosity of the solvent and  $\phi$  is the volume fraction of the dispersed phase that is surfactant and water. This is really the situation. It is therefore clear that the viscosity must fall from a value of 450 mPa·s at 10% of oil to a low value at 50%. It is, however, not clear why the viscosity decreases so strongly between 10 and 50%. Perhaps the reason could be of electrostatic origin.

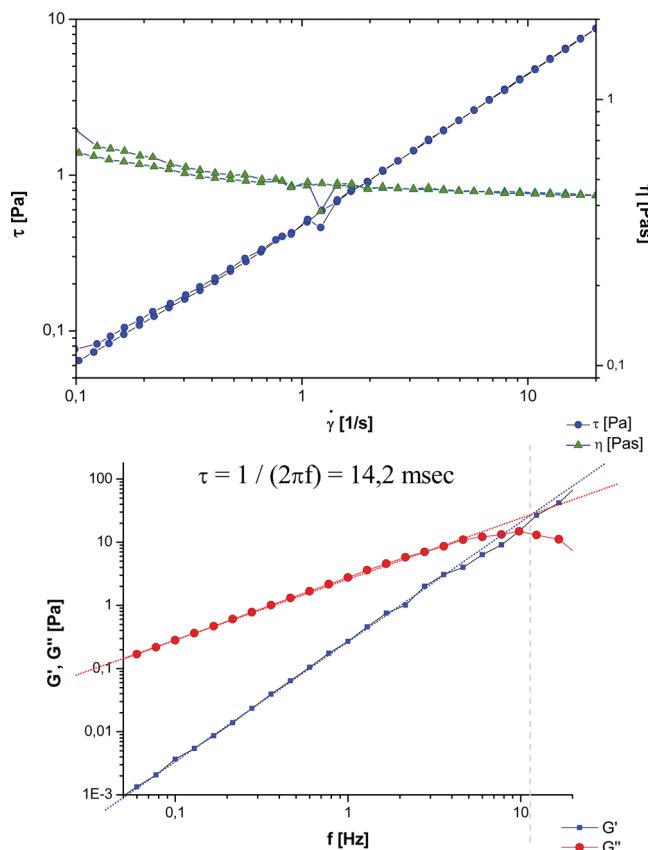


**Figure 9.** Rheograms of microemulsion from upper single phase channel with 6% oil in the solvent mixture. Top: shear stress  $\tau$  and viscosity  $\eta$  against shear rate  $\dot{\gamma}$ ; bottom: storage modulus  $G'$  and loss modulus  $G''$  against frequency  $f$ . Evaluated structural relaxation time: 14.2 ms.

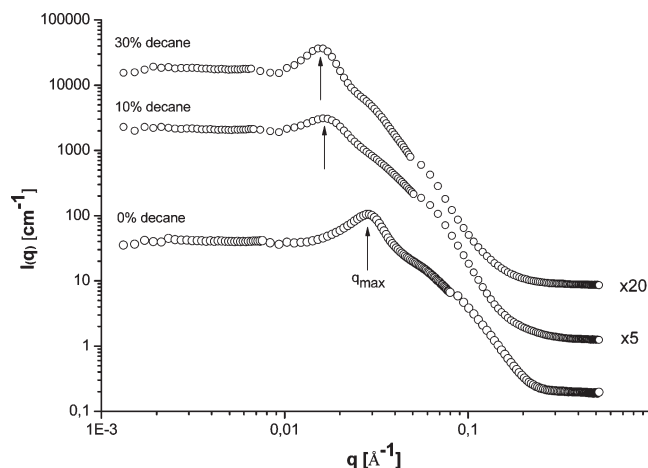


**Figure 10.** SANS experiment at constant surfactant concentration with increasing mass fraction of oil in the solvent. For better overview, curves for microemulsions with 10 and 30% decane are shifted by factors of 5 and 20 on the intensity scale.

In any event, the maximum of the viscosity also stands for a transition in the nanostructure around this oil content.

The viscosity of a structured fluid is in the simplest case determined by the product of a shear modulus and a relaxation

**Table 1.** Data Obtained from SANS Measurements:  $q_{\max}$  Values and Calculated Interlamellar Distance  $d$  at Constant Surfactant Concentration in Dependency of Increasing Mass Fraction of Decane in the Solvent Mixture

surfactant (%)	$x$ IT 3	$x$ decane	$q_{\max}$ ( $\text{\AA}^{-1}$ )	$d$ ( $\text{\AA}^{-1}$ )
15	0.795	0	0.02895	217
15	0.635	0.1	0.01619	388
15	0.74	0.3	0.01521	413

time ( $\eta^o = G^o \cdot \tau$ ). This is the situation in  $L_1$  phases of micellar solutions. We tried therefore to determine the structural relaxation time  $\tau_s$  of the samples around the viscosity maximum.

In Figure 9, we show in a plot of the shear viscosity of the microemulsion at the viscosity maximum against the shear rate and results from oscillating measurements of the complex viscosity against the angular frequency. Both Figures show the typical results for shear thinning liquids. With help of oscillating measurements, the relaxation time can be evaluated. The value is 14 ms. This value of 14 ms is the same as the time constant that was evaluated as the longest process from the electric birefringence measurements. We therefore can conclude that the longest time constant, which is determined from electric birefringence results on the microemulsions, is the structural relaxation time of the fluid, which controls the viscosity.

**SANS Measurements in the Upper Single-Phase Channel.** Intuitively, it is difficult to understand why the viscosity or the structural relaxation times are increasing so much when 10% of oil is solubilized into the  $L_3$  phase. An answer of this puzzling question can be obtained from SANS measurements that have been made on the  $L_3$  phase and on microemulsions from the upper channel with varying oil content (Figure 10).

The result for the sample without decane shows the typical scattering function for an  $L_3$  phase. However, a shift is observed between the correlation peak of the  $L_3$  phase and the correlation peak of the microemulsion with 10% of oil to a lower  $q$  value. The  $q$  value for the microemulsion with 30% decane is similar to the microemulsion with 10% decane.

Whereas the calculated interlamellar distance of the  $L_3$  phase is  $\sim 22$  nm, the sample with 10% decane shows an interlamellar distance of  $\sim 39$  nm (Table 1). These results show clearly that between the  $L_3$  phase without oil and the microemulsions with 10% of oil a massive structural reorganization must have taken place, whereas between 10 and 30% of decane the structure keeps mainly the same.

The SANS data are in good agreement with the results obtained by the FF-TEM micrographs. The interlamellar distance of the  $L_3$  phase is in the same range, as can be seen on the FF-TEM micrograph in Figure 3. The obtained  $d$  values for the sample with 10 and 30% decane also correspond to the size of the globular particles that were seen on the micrograph for the microemulsion with 20% decane and could represent the droplet diameter. It is also noteworthy that the scattering curve for the sample with 10% decane does have a broader peak that is not as sharp as for the other two curves. This could mean that there is a larger polydispersity in the size distribution of the w/o droplets or some of them are fused together. Because the structural relaxation time is related to the deformation of the correlation peak, it is not surprising that the structural relaxation time increases strongly with the solubilization because the sample consists probably of densely packed droplets. There might be a

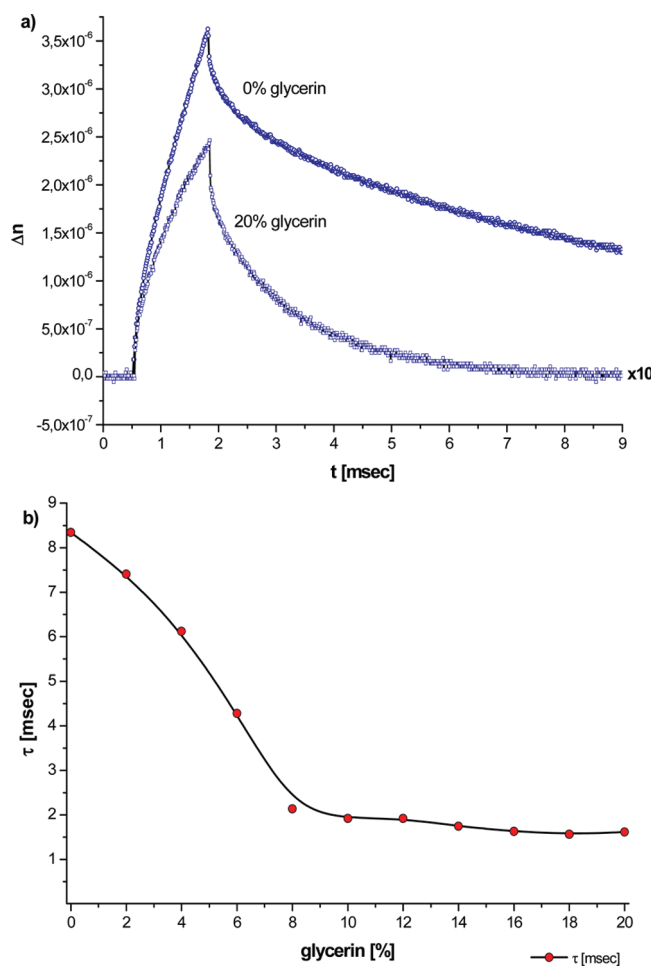


**Figure 11.** Dependence of structural relaxation time on solvent viscosity. (a) EB signals of microemulsions from the upper channel with 20% decane in solvent and different glycerin content recorded at a field strength of 133 kV/m. The curve for the microemulsion with 20% glycerin in water was increased by a factor of 10 for better overview. (b) Relaxation time  $\tau$  in dependence of glycerin concentration of a microemulsion of the upper single-phase channel with 20% decane in the solvent mixture.

second reason for the increase in the structural times. As shown from the phase diagram of Figure 1, samples with 10% oil have a higher content of  $Mg(DS)_2$  than samples of the  $L_3$  phase. The ionic charge density of the samples is considerably higher than that for the  $L_3$  phase. This increase probably leads to a stiffening of the bilayer and also to an increase in the time constants. Qualitatively, this effect should lead to a stronger correlation peak and a stronger interbilayer interaction.

The data differ completely from SANS-measurements that were done on microemulsions with the single nonionic surfactant  $C_{12}E_5$  and decane. In these results, the  $q_{\max}$  values did not shift with constant surfactant and increasing solubilization of oil into the  $L_3$  phase, assuming that the interlamellar distance and the structure of the  $L_3$  phase do not change.<sup>29</sup>

**Dependence of the Structural Relaxation Time on the Solvent Viscosity.** The signals of the birefringence results of the  $L_3$  phase were explained by the rotation of disks in the aqueous medium. For such a mechanism, the relaxation time should be proportional to the solvent viscosity. Some measurements were carried out on a microemulsion in which up to 20% of water was

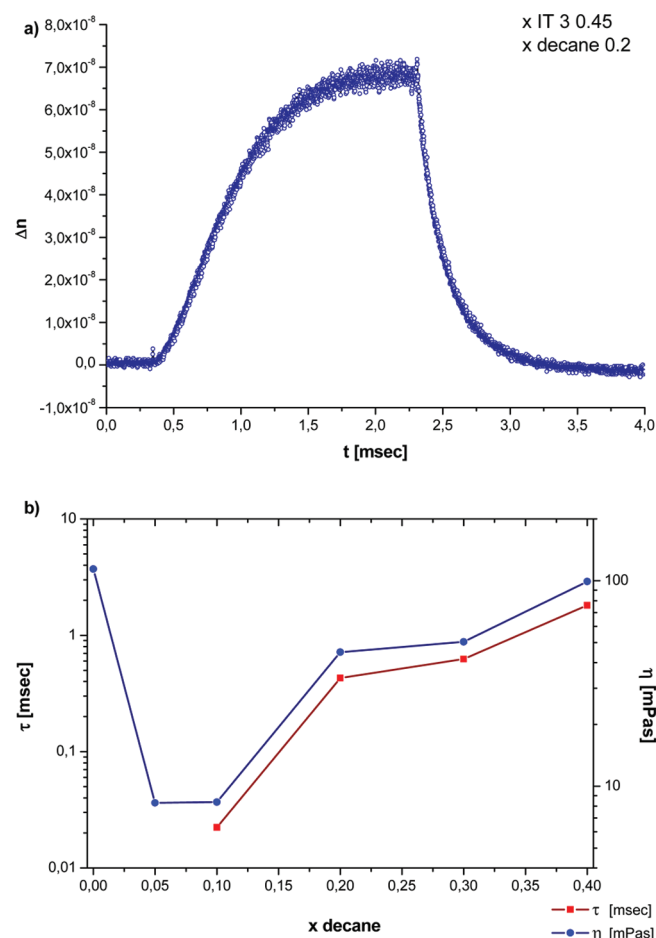


**Figure 12.** Results of electric birefringence in the lower single phase channel. (a) EB signal of microemulsion from the lower single phase channel with 20% decane in the solvent mixture. (b) Overview of main structural relaxation time and zero shear viscosity with increasing oil content in the lower single phase channel.

replaced by glycerin. Two signals, one with water and one with 20% of glycerin, are shown in Figure 11a. At first, it is remarkable that the intensity  $\Delta n$  of the sample with 20% glycerin is much lower than the intensity of the sample without glycerin. This is probably caused by matching the refractive index of the aqueous phase against the oil and also can be clearly seen by eye. Whereas the sample without glycerin scatters much and is somewhat bluish, the sample with 20% glycerin scatters less.

The signals also clearly show that the time constants indeed depend on the glycerin content. With increasing glycerin concentration, the structural time constants become shorter and not longer as expected, as can be seen in Figure 11b.

It can therefore be concluded that the relaxation times are not only determined on the viscosity of the solvent but also depend on the stiffness of the bilayers and perhaps on the interaction energy between the bilayers. Whereas the observed change of the structural relaxation time with the glycerin content is surprising, we would like to add that the change is similar to the change that has been observed on the structural relaxation time of  $L_1$  phases with wormlike micelles.<sup>30</sup> In this case, the decrease in the structural relaxation times can be understood on the basis of the reptation mechanism for the wormlike micelles. Perhaps the relaxation

process in the investigated microemulsions is a similar process to the reptation mechanism in a L<sub>1</sub> phase.

**Dynamic Behavior in the Lower Channel.** EB signals also were recorded for the microemulsions of the lower single phase channel. A selected signal for samples with 20% decane is shown in Figure 12a. Signals from 10 to 40% decane are shown in Figure SI9 of the Supporting Information. The signals for microemulsions in the lower channel are far simpler than the signals from the upper channel.

The viscosities and the structural relaxation times in the lower channel are given in Figure 12b. For no oil, the viscosity has a value of  $\sim 110$  mPas. This value indicates that the micellar solution contains entangled wormlike micelles. With increasing solubilization, the viscosity passes through a deep minimum around 5% of oil and then increases again with increasing solubilization of oil. The decrease in the viscosity is an indication that the wormlike micelles have been transformed to small oil droplets. The transition of wormlike micelles to globular droplets by the solubilization of oil has already been studied in detail.<sup>31</sup> It occurs rather sharp, and the transition concentration of oil depends on its chain length. Wormlike micelles of a given surfactant can tolerate small hydrocarbon molecules more than long ones before they are transformed to globular droplets. It is interesting to note that the minimum of the viscosity in the lower channel coincides with the maximum of the viscosity in the upper channel. It is furthermore interesting that the globular micelles give rise to an electric birefringence signal even though the particles are not anisotropic. FF-TEM measurements in Figure 3 showed that the particles are perfect spheres. The reason for the electric birefringence signal is the same as that for the signal in the L<sub>3</sub> phase. The droplets obviously are deformed in the electric field. The deformation seems to be small, as is evidenced by the validity of Kerr's law up to high electric fields.

The electrostatic interaction between the droplets does not seem to influence very much their rotation. If a radius for the droplets is determined from the time constant of the birefringence signals and it is assumed that this time constant is given approximately by the rotation of the droplets, then one obtains a radius that is close to the radius that is obtained from FF-TEM measurements.

With increasing solubilization of oil, the globular droplets increase in size and the viscosity and the structural relaxation time. Both parameters seem to be affected now more and more by the interaction of the particles, either hydrodynamic or electrostatic in origin.

The system is becoming denser with increasing solubilization. At maximum solubilization around 40% decane, the viscosity and the structural relaxation time of the samples are now higher than those for samples with 40% of decane in the upper channel.

## CONCLUSIONS

Electric birefringence measurements give strong signals in the isotropic channel of microemulsions in the region where a bicontinuous structure exists and in the regions where w/o or o/w droplets exist. The signals are due to the deformation of the nanostructures in the electric field. It is shown in the investigation that the longest relaxation time that is evaluated from the electric birefringence signals controls the viscosity of the fluids in the channel. The structural relaxation times and the viscosities of the upper single-phase channel pass with increasing oil content over a strong maximum. The position of the viscosity maximum

occurs at  $\sim 10\%$  of oil. It is concluded that the viscosity maximum is the result of switch in the nanostructure from a low viscous flexible L<sub>3</sub> phase to a densely packed w/o-HIPE structure. Between 1 and 10% of oil, the EB signals become very complicated because they show a superposition of up to three processes. The complicated signals are due to a complex transition mechanism from a bicontinuous L<sub>3</sub> phase to a w/o-HIPE structure. For higher oil content, EB signals become less complicated, which indicates a completion of the structural transition. The structural relaxation times are decreasing with increasing oil content because of the decreasing droplet size of the w/o droplets. All in all, the longest relaxation time seems to control the viscosity of the fluids. Results of the electric birefringence measurements are supported by conductivity measurements, FF-TEM micrographs, and SANS measurements.

## ASSOCIATED CONTENT

**S Supporting Information.** More information, as detailed rheology measurements in the lamellar channel and electric birefringence signals along the microemulsion channels. This material is available free of charge via the Internet at <http://pubs.acs.org>.

## AUTHOR INFORMATION

### Corresponding Author

\*Tel: +49-921-50736168. Fax +49-921-50736139. E-mail: lukas.wolf@freenet.de.

## ACKNOWLEDGMENT

We thank Dr. Walter Richter at the Centre for Electron Microscopy, Jena, for the great FF-TEM imaging work and Dieter Gräbner for his eager assistance in operating the electric birefringence device. We also want to thank the group of Prof. Dr. Thomas Hellweg, University of Bielefeld, for the possibility to investigate samples by SANS-measurements at the Institute Laure-Langevin (ILL) in Grenoble, France.

## REFERENCES

- (1) Miller, C. A.; Neogi, P. *AIChE J.* **1980**, *26*, 212–220.
- (2) Huang, J. S. *J. Chem. Phys.* **1985**, *82*, 480–484.
- (3) Strey, R. *Colloid Polym. Sci.* **1994**, *272*, 1005–1019.
- (4) Lee, L. T.; Langevin, D.; Strey, R. *Physica A* **1990**, *168*, 210–290.
- (5) Sottmann, T.; Strey, R. *J. Chem. Phys.* **1997**, *106*, 8606–8615.
- (6) Stubenrauch, C. In *Microemulsions: Background, New Concepts, Applications, Perspectives*; Wiley-Blackwell: Chichester, U.K., 2009.
- (7) Lichtenfeld, F.; Schmeling, T.; Strey, R. *J. Phys. Chem.* **1986**, *90*, 5762.
- (8) Wolf, L.; Hoffmann, H.; Watanabe, K.; Okamoto, T. *Phys. Chem. Chem. Phys.* **2011**, *13*, 3248–3256.
- (9) Khan, A.; Lindström, B.; Shinoda, K.; Lindman, B. *J. Phys. Chem.* **1986**, *90*, 5799.
- (10) Kahlweit, M. *J. Colloid Interface Sci.* **1987**, *118*, 436–453.
- (11) Jahn, W.; Strey, R. *J. Phys. Chem.* **1988**, *92*, 2294.
- (12) Hoffmann, H.; Horbaschek, K.; Witte, F. *J. Colloid Interface Sci.* **2001**, *235*, 33–45.
- (13) Hoffmann, H.; Thunig, C.; Munkert, U.; Meyer, H. W.; Richter, W. *Langmuir* **1992**, *8*, 2629–2638.
- (14) Douglas, C. B.; Kaler, E. W. *J. Chem. Soc., Faraday Trans.* **1994**, *90*, 471–477.
- (15) Wolf, L.; Hoffmann, H.; Talmon, Y.; Teshigawara, T.; Watanabe, K. *Soft Matter* **2010**, *6*, 5367–5374.

- (16) Schorr, W.; Hoffmann, H. *Physics of Amphiphiles: Micelles, Vesicles and Microemulsions: Proceedings of the International School of Physics*; Degiorgio, V., Corti, M., Eds.; North-Holland: Amsterdam, 1985; pp 160–180.
- (17) Krämer, U.; Hoffmann, H. *Macromolecules* **1991**, *24*, 256–263.
- (18) Hoffmann, H.; Krämer, U.; Thurn, H. *J. Phys. Chem.* **1990**, *94*, 2027–2033.
- (19) Stellwagen, N. C. *Biopolymers* **1991**, *31*, 1651–1667.
- (20) Miller, C. A.; Gradzielski, M.; Hoffmann, H.; Krämer, U.; Thunig, C. *Prog. Colloid Polym. Sci.* **1991**, *84*, 243.
- (21) Cates, M. E.; Roux, D. *J. Phys.: Condens. Matter* **1990**, *2*, 339–346.
- (22) Strey, R.; Jahn, W.; Skouri, M.; Porte, G.; Marignan, J.; Olsson, U. In *Structure and Dynamics of Strongly Interacting Colloids and Supramolecular Aggregates in Solution*; Chen, S. H., Huang, J. S., Tartaglia, P., Eds.; Kluwer Academic: Boston, 1992; pp 351–363.
- (23) Porte, G.; Appel, J.; Bassereau, P.; Marignan, M.; Skouri, M.; Billard, J.; Delsanti, M.; Candau, S. J.; Jahn, J.; Nabre, P. *Prog. Colloid Polym. Sci.* **1991**, *84*, 264.
- (24) Kahlweit, M.; Strey, R.; Haase, D.; Kunieda, H.; Schmelting, T.; Faulhaber, B.; Borkovec, M.; Eicke, H. F.; Busse, G.; Eggers, F.; Funck, T.; Richmann, H.; Magid, L.; Soderman, O.; Stilbs, P.; Winkler, J.; Dittrich, A.; Jahn, W. *J. Colloid Interface Sci.* **1987**, *118*, 445.
- (25) Miller, C.; Gradzielski, M.; Hoffmann, H.; Krämer, U.; Thunig, C. *Colloid Polym. Sci.* **1990**, *268*, 1066–1072.
- (26) Krämer, U.; Hoffmann, H. In *The Structure, Dynamics, and Equilibrium Properties of Colloidal Systems*; Bloor, D. M., Wyn-Jones, E., Eds.; NATO ASI Series: Series C, Mathematical and Physical Sciences 324; Kluwer Academic Publishers: Boston, 1990; pp 385–396.
- (27) Yamaguchi, Y.; Hoffmann, H. *Colloids Surf., A* **1997**, *121*, 67–80.
- (28) Kahlweit, M.; Strey, R.; Haase, D.; Kunieda, H.; Schmelting, T.; Faulhaber, B.; Borkovec, M.; Eicke, H. F.; Busse, G.; Eggers, F.; Funck, T.; Richmann, H.; Magid, L.; Soderman, O.; Stilbs, P.; Winkler, J.; Dittrich, A.; Jahn, W. *J. Colloid Interface Sci.* **1987**, *118*, 443–444.
- (29) Uhrmeister, P. *Selbstorganisierende Netzweke in Mikroemulsionen*. Ph.D. Thesis, Universität Köln, 2002.
- (30) Hoffmann, H.; Abdel-Rahem, R. *Colloid Polym. Sci.* **2010**, *288*, 603–612.
- (31) Hoffmann, H.; Ulbricht, W. *J. Colloid Interface Sci.* **1989**, *129*, 388–405.
- (32) Licherfeld, F.; Schmelting, T.; Strey, R. *J. Phys. Chem.* **1986**, *90*, 5762–5766.